CSIRO PUBLISHING

Australian Journal of Chemistry

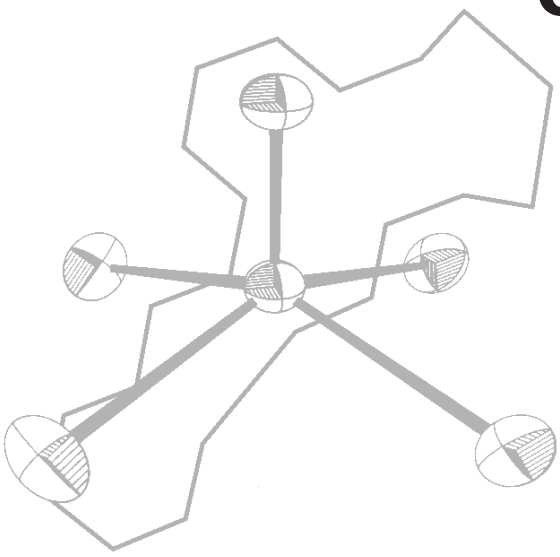

Volume 53, 2000

A journal for the publication of original research
in all branches of chemistry and chemical technology

www.publish.csiro.au/journals/ajc

All enquiries and manuscripts should be directed to
The Managing Editor
Australian Journal of Chemistry
CSIRO PUBLISHING
PO Box 1139 (150 Oxford St)
Collingwood Telephone: 61 3 9662 7630
Vic. 3066 Facsimile: 61 3 9662 7611
Australia Email: john.zdysiewicz@publish.csiro.au

Published by **CSIRO** PUBLISHING
for CSIRO and
the Australian Academy of Science

Aust. J. Chem., 2000, **53**, 355–361

Selective On-Resonance N.M.R. Irradiation of a Dipolar Doublet*

Frances Separovic,[A] *Nikolai R. Skrynnikov*[B] *and Bryan C. Sanctuary*[B]

[A] School of Chemistry, University of Melbourne, Vic. 3010.
Author to whom correspondence should be addressed. Phone: 03 8344 6464.
Fax: 03 9347 5180. E-mail: f.separovic@chemistry.unimelb.edu.au
[B] Department of Chemistry, McGill University, Montreal, Quebec, Canada H3A 2K6.

Raman magnetic resonance where double-quantum transitions are observed without the need for multidimensional n.m.r. spectroscopy has been investigated further. Theoretical analysis of the on-resonance case where weak continuous-wave irradiation was applied at the frequency of a single-quantum transition was performed and guidelines for a consistent perturbation treatment were devised. Theoretical results agree well with experimental data obtained for a system of two dipolar coupled nuclei of spin ½ oriented by a liquid crystal. The same approach is applicable to near-resonance experiments which are shown to be the optimal experimental scheme for Raman n.m.r. By using weak selective irradiation, a symmetric excitation–detection scheme can be realized for multiple-quantum n.m.r. experiments. Near- or on-resonance selective irradiation provides an efficient transfer of multiquantum coherence into observable coherences and could be used to study multiquantum relaxation processes.

Keywords: Multiple-quantum n.m.r.; Raman n.m.r.; selective excitation; operator basis; multipole representation; dipolar coupling; difluorotetrachloroethane.

Introduction

Modern n.m.r. techniques often involve the observation of multiple-quantum (MQ) transitions.[1] The interpretation of combined single-quantum (1Q) and MQ data allows the refinement of structural information and avoids some ambiguities inherent in 1Q spectra. Moreover, the observation of MQ relaxation complements 1Q relaxation data, allowing for the extraction of motional parameters and for the probing of weak relaxation mechanisms.[1]

The standard method for recording of MQ transitions is provided by two-dimensional (2D) n.m.r. techniques. This method involves a number of experiments where the multiquantum coherence is produced in the course of a preparation period and subsequently evolves during an evolution period t_1. This is incremented parametrically from experiment to experiment, while in the mixing period MQ coherences are transformed into observable 1Q coherences which are recorded during the detection period. Fourier transformation of the response with respect to t_1 yields the sought-for MQ spectrum. Such 2D experiments, however, consume time and data-storage capacity.

In contrast to MQ multidimensional n.m.r., experiments directed toward the investigation of MQ relaxation do not require multidimensional mapping. The recording of the MQ lines in relaxation experiments can be performed using a single-shot measurement such as conventional slow-passage techniques.[2,3] The multiquantum signals appear in a slow-passage spectrum, while a system is being irradiated in continuous-wave (CW) mode by an r.f. field, at frequency:

$$\omega_{rf} = (E_a - E_b)/p_{ab} \qquad (1)$$

where E_a and E_b are the energy levels of the spin system and $p_{ab} = M_a - M_b$ is the order of the transition. Note that for a system of two coupled spins ½ the double-quantum line appears at the centre of the doublet lines. It is recognized, however, that the use of the conventional CW approach for observation of MQ transitions is subject to a number of experimental difficulties.[4] These may be overcome with a cross-coil arrangement.[5]

The experiment by Yannoni *et al*.[5] can be considered a development of the slow-passage CW technique. The distinctions are as follows. Firstly, the r.f. frequency is shifted from the position given by equation (1). The use of shifted carrier frequency is typical for modern n.m.r. experiments. Secondly, r.f. irradiation is not used to excite MQ coherences, rather a preparation period is introduced in analogy with 2D methods in order to produce MQ coherences. Thirdly, the spectrum is obtained as the Fourier transform of the response signal acquired as the system is exposed to continuous irradiation at a fixed frequency.

The coherence $\hat{\rho}_{ab}$ formed by two arbitrary states $|a\rangle$ and $|b\rangle$ evolves in the rotating frame according to

$$\hat{\rho}_{ab}(t) = \hat{\rho}_{ab}(0) \exp[-i(E_a - E_b + p_{ab}\omega_{rf})t] \exp(-t/T_2^{ab}) \qquad (2)$$

* Dedicated to Professor Don Cameron on the occasion of his 65th birthday. Professor Cameron's continuing enjoyment in undergraduate teaching and his concern for students has been inspiring.

Manuscript received 21 March 2000 10.1071/CH00044 0004-9425/00/040355

This formula implies a characteristic dependence of the apparent frequencies on the carrier frequency ω_{rf}. Whenever the carrier frequency is shifted by $\Delta\omega_{rf}$, the MQ transition frequencies shift by $p_{ab}\Delta\omega_{rf}$ relative to the frequency origin of the rotating frame. This property is used in multidimensional n.m.r. to separate MQ signals of different order.[1]

In analogy with Raman spectroscopy, Yannoni's experimental technique involves continuous irradiation of the system at the fixed frequency while simultaneously detecting the response. A double-quantum (2Q) process takes place with $\Delta M = 2$, suggesting the term Raman n.m.r. As with traditional CW technique, Raman n.m.r. has similar disadvantages, such as frequency shifts arising from the interaction with the r.f. field but, like 2D methods, the data acquisition period combines free evolution of MQ coherences and their simultaneous transformation to observable coherences (mixing).

In the original Raman experiment,[5] a double-quantum transition is observed using two dipolar coupled spins ½ of the identical ^{19}F nuclei in difluorotetrachloroethane aligned in a nematic liquid crystal. Theoretical treatment for this experiment was first presented by Bowden and coworkers.[6] A system of two dipolar coupled spins ½ is equivalent in this case to a spin $I = 1$ evolving under an axially symmetric quadrupole interaction. The preparation sequence $(\pi/2)_x$–τ–$(\pi/2)_x$, where τ is a matched preparation delay, is intended to bring the system to a state containing solely 2Q coherences. As the system evolves from those initial conditions, the detectable signal $\langle I_- \rangle \propto (\hat{\rho}_{-10}+\hat{\rho}_{01})$ includes a component, corresponding to the 2Q transition:[6]

$$(\hat{\rho}_{-10}+\hat{\rho}_{01}) \propto \ldots + [\omega_1\omega_Q/\delta\omega] \exp[i(2\Delta\omega - \omega_1^2\,\Delta\omega/\delta\omega)t] + \ldots \quad (3)$$

where $\delta\omega = \omega_Q^2 - \Delta\omega^2$. Here ω_Q stands for the parameter of the effective quadrupolar Hamiltonian (corresponding to a residual dipolar splitting), ω_1 gives the intensity of the applied r.f. field and $\Delta\omega$ is the offset of the carrier frequency: $\Delta\omega = \omega_{rf} - \omega_0$. This result is derived by Bowden *et al.*[6] using perturbation theory for non-degenerate states. As seen from equation (3), this result fails if $\delta\omega = 0$ or $\Delta\omega = \pm\omega_Q$, i.e., if the r.f. field is applied to one of the lines of a spin $\mathbf{I} = 1$ doublet. Although the on-resonance case, $\Delta\omega = \pm\omega_Q$, is discussed separately in a subsequent paper by Bowden *et al.*,[7] the case is not solved exactly. In both works[6,7] the spherical tensor basis is used to represent the density matrix. The use of spherical tensors leads to an inconvenient form of the Liouville operator (i.e., the matrix of the Liouville operator is off-diagonal with respect to ω_Q)[6] but, if the evolution of the system is treated in Hilbert space, then the spherical tensor basis provides a natural form for the resulting density matrix.[6,7]

Following this, Yang and Ye[8,9] reported the results of Raman n.m.r. experiments performed for *AX* and AX_n systems and demonstrated the application of Raman n.m.r. to relaxation measurements[10] which could be considered the primary application of this technique. For the case of an *AX* system[3] it is shown that for strong r.f. fields $\omega_1 \geq \omega_Q$ the intensity of the observed 2Q response decreases rapidly as the field strength ω_1 increases. For an A_2 system this can be simply explained, since intensive r.f. irradiation leads to spin decoupling and 2Q coherence tends to disappear under such conditions.[11] In view of this effect we can infer that a properly adjusted Raman n.m.r. experiment should use a weak probing field $\omega_1 \leq \omega_Q$, since the goal of Raman n.m.r. is the observation of MQ coherences. Therefore, a weak probing field is essentially inherent in Raman n.m.r. experiments and ω_1 can be consistently treated as a perturbation. Thus, the consequent application of perturbation theory covering the on-resonance case $\Delta\omega = \pm\omega_Q$, where degenerate state theory should be invoked, is important for the theoretical description of Raman n.m.r. The analysis to be presented in this article is aimed at this specific problem.

As noted above, the variation of the carrier offset $\Delta\omega$ is used to shift the MQ signals of different order relative to one other in the observed spectrum. In the on-resonance case, $\Delta\omega = \pm\omega_Q$, the double-quantum line proves to be superimposed on one single-quantum line while the zero-quantum line is superimposed on the other single-quantum line. Under these conditions the 2Q coherence of order $p = -2$ that is produced during the preparation period is efficiently transferred to observable 1Q coherence and the observed signal is thus a manifestation of the intermixed evolution of 1Q and 2Q coherences.

The theoretical treatment of the on-resonance irradiation experiment is presented below and the results are subsequently used to interpret the experimental data obtained for difluorotetrachlorethane aligned in a nematic liquid crystal. This is the same dipolar coupled system used in the original Raman n.m.r. experiment[5] and examining such effects is relevant in modern n.m.r. structural studies which measure residual dipolar couplings in solution and in aligned systems.[12]

Theory

As discussed by Keller[13] two dipolar coupled, identical spin ½ nuclei can be considered as an $\mathbf{I} = 1$ spin system, evolving under an axially symmetric quadrupole interaction. Selective excitation of such a spin system has been detailed by Sanctuary[11] for the special case where $\omega_1 \gg \omega_Q$. In addition, the evolution of the $\mathbf{I} = 1$ spin system for weak r.f. field, $\omega_1 \ll \omega_Q$, has been examined[14,15] using fictitious spin ½ operators. In this section we treat the case of weak, selective excitation applied on-resonance with one of the 1Q transitions ($\Delta\omega = \pm\omega_Q$, i.e., one of the doublet lines is irradiated), and the r.f. field directed along the *x* axis in the rotating frame. A general scheme for the experiment is given by the sequence $(\pi/2)_x$–τ_1–$(\pi/2)_x$–t. The preparation period consists of two $(\pi/2)$ pulses separated by delay τ_1 which is set approximately equal to $\pi/2\omega_Q$ in order to parallel the original 2Q Raman n.m.r. experiment. During the subsequent period t the system is exposed to weak CW irradiation and the response is recorded simultaneously.

During the detection period, t, the Hamiltonian can be written in the form:

$$\mathbf{H} = -\omega_0\mathbf{I}_z + \omega_Q[3\mathbf{I}_z^2 - \mathbf{I}(\mathbf{I}+1)]/3\mathbf{I}(2\mathbf{I}-1) + \tfrac{1}{2}\omega_1 \exp(i\varpi_{rf} t)\mathbf{I}_+ - \tfrac{1}{2}\omega_1 \exp(i\varpi_{rf} t)\mathbf{I}_- \quad (4)$$

where $\varpi_{rf}\,t = \omega_{rf}t+\phi$. Our task is to obtain an explicit expression for the density matrix evolving under the Hamiltonian of equation (4). In the $|M\rangle\langle M'|$ basis, the quantum Liouville equation[16] can be written in the form:

$$i(d/dt)\{\rho_{MM'}(t)\} =$$

$$\Sigma_{MM'}\,\mathrm{Tr}\{(|M\rangle\langle M'|)^{\dagger}\,[\mathbf{H}, |M\rangle\langle M'|]_{-}\}\rho_{MM'}(t) \qquad (5)$$

The Zeeman and quadrupolar terms of Hamiltonian (4) are diagonal in the $|M\rangle\langle M'|$ basis, and the r.f. term can be treated as a perturbation. In a frame rotating with the carrier frequency ω_{rf} the density matrix components are related to those of the laboratory frame via:

$$\hat{\rho}_{MM'}(t) = \exp[-i(M-M')(\varpi_{rf}\,t)]\,\rho_{MM'}(t) \qquad (6)$$

Using equations (4)–(6) we obtain the equation for the density matrix evolution in this rotating frame:

$$\begin{aligned} i(d/dt)\{\hat{\rho}_{MM'}(t)\} = \\ &[\Delta\omega(M-M') + \omega_Q(M^2-M'^2)/\mathbf{I}(2\mathbf{I}-1)]\,\hat{\rho}_{MM'}(t) \\ &+\tfrac{1}{2}\,\omega_1[(\sqrt{\{(\mathbf{I}+M)(\mathbf{I}-M+1)\}})\hat{\rho}_{M-1M'}(t) \\ &+(\sqrt{\{(\mathbf{I}-M)(\mathbf{I}+M+1)\}})\hat{\rho}_{M+1M'}(t) \\ &-(\sqrt{\{(\mathbf{I}-M')(\mathbf{I}+M'+1)\}})\hat{\rho}_{MM'+1}(t) \\ &-(\sqrt{\{(\mathbf{I}+M')(\mathbf{I}-M'+1)\}})\hat{\rho}_{MM'-1}(t)] \end{aligned} \qquad (7)$$

where $\Delta\omega = \omega_{rf} - \omega_0$. The r.f. frequency ω_1 appears here in a modified form being multiplied by square root factors.[17] This gives the effective r.f. frequencies observed in selective experiments. Note that this equation is valid for all $\mathbf{I}$ and all $\Delta\omega$. We restrict ourselves, however, to the case $\mathbf{I} = 1$ and $\Delta\omega = \omega_Q$, i.e., on-resonance irradiation of a high-field line of the doublet. In this case equation (7) takes the explicit form:

$$i(d/dt)\{\hat{\boldsymbol{\rho}}(t)\} = \boldsymbol{M}\,.\,\hat{\boldsymbol{\rho}}(t) \qquad (8)$$

with matrix $\boldsymbol{M}$ equal to:

$$\begin{pmatrix}
0 & -\varpi_1 & \varpi_1 & 0 & 0 & -\varpi_1 & 0 & \varpi_1 & 0 \\
-\varpi_1 & 0 & 0 & \varpi_1 & 0 & 0 & 0 & 0 & \varpi_1 \\
\varpi_1 & 0 & 0 & -\varpi_1 & 0 & 0 & -\varpi_1 & 0 & 0 \\
0 & \varpi_1 & -\varpi_1 & 0 & 0 & 0 & 0 & 0 & 0 \\
0 & 0 & 0 & 0 & 0 & \varpi_1 & 0 & -\varpi_1 & 0 \\
-\varpi_1 & 0 & 0 & 0 & \varpi_1 & -2\omega_Q & \varpi_1 & 0 & 0 \\
0 & 0 & -\varpi_1 & 0 & 0 & \varpi_1 & -2\omega_Q & 0 & 0 \\
\varpi_1 & 0 & 0 & 0 & -\varpi_1 & 0 & 0 & 2\omega_Q & -\varpi_1 \\
0 & \varpi_1 & 0 & 0 & 0 & 0 & 0 & -\varpi_1 & 2\omega_Q
\end{pmatrix} \qquad (9)$$

where $\varpi_1 = \omega_1/\sqrt{2}$ and vector $\boldsymbol{\rho}$ is composed from $\rho_{MM'}$ elements arranged in the following order: ρ_{00}, ρ_{0-1}, ρ_{-10}, ρ_{-1-1}, ρ_{11}, ρ_{01}, ρ_{-11}, ρ_{10}, ρ_{1-1}. Note that $\boldsymbol{M}$ is diagonal in ω_Q, and off-diagonal in ω_1 by virtue of the $|M\rangle\langle M'|$ basis. Exact solution for this set of coupled first-order differential equations is given by:

$$\hat{\boldsymbol{\rho}}(t) = (\boldsymbol{U}\exp[-i\boldsymbol{D}t]\,\boldsymbol{U}^{-1})\hat{\boldsymbol{\rho}}(0) \qquad (10)$$

where $\boldsymbol{D}$ is obtained by diagonalization of $\boldsymbol{M}$, and $\boldsymbol{U}$ specifies the corresponding unitary transformation:

$$\boldsymbol{D} = \boldsymbol{U}^{-1}\boldsymbol{M}\,\boldsymbol{U} \qquad (11)$$

Equation (10) can be rewritten in a more convenient form for each density matrix element ρ_k, where the index k is used for the pair of indices M, M'. The density matrix can thus be interpreted as a vector in Liouville space:

$$\hat{\boldsymbol{\rho}}_{\boldsymbol{k}}(t) = \Sigma\,\{(\boldsymbol{\eta}^j\,.\,\boldsymbol{\sigma}^k)\,(\boldsymbol{\eta}^j\,.\,\hat{\boldsymbol{\rho}}(0))\}\,\exp(-i\lambda_j\,t) \qquad (12)$$

Here $\boldsymbol{\eta}^j$ stands for jth eigenvector of $\boldsymbol{M}$, $\boldsymbol{\sigma}^k$ denotes the vector with only non-zero element $\sigma^k{}_i = \delta_{ik}$, $\boldsymbol{\rho}(0)$ is the vector describing the initial conditions and $(\alpha\,.\,\beta)$ corresponds to the scalar product of two vectors. The exact eigenvalues of the matrix $\boldsymbol{M}$ that enter equation (12) are tabulated in Appendix A.

In equation (12) the sum is constructed in such a way that the evolution of the density matrix is represented as a set of quantum beats $\exp[-i\lambda_j t]$, and the factors $\{(\boldsymbol{\eta\sigma})(\boldsymbol{\eta\rho})\}$ are responsible for the intensity of the corresponding beats. Equation (10) permits an alternative representation,* where the density matrix is expressed as a set of evolving initial components $\rho_j(0)$.

The result (12) is exact. As it was noted above, however, a properly adjusted Raman experiment is adequately described within the framework of perturbation theory. Thus, the exact eigenvalues and eigenvectors in equation (12) can be substituted for approximations, obtained by use of perturbation theory of appropriate order. In the present case, ordinary perturbation theory cannot be used because of the degeneracies in $\boldsymbol{M}$. In order to apply a perturbation approach for degenerate states,[18,19] we define in $\boldsymbol{M}$ the block-diagonal part $\boldsymbol{M}_{BD}$, where the blocks relate to the subsets of $\rho_{MM'}$ with degenerate diagonal value of $\boldsymbol{M}_{MM',MM'}$ cross-linked with off-diagonal elements:

$$i(d/dt)\{\hat{\boldsymbol{\rho}}(t)\} = (\boldsymbol{M}_{BD} + \boldsymbol{M'})\,\hat{\boldsymbol{\rho}}(t) \qquad (13)$$

Here the matrix $\boldsymbol{M}'$ represents the ω_1 perturbation between the blocks.

The first step in the application of perturbation theory is the diagonalization of $\boldsymbol{M}_{BD}$, yielding the first-order approximations for the eigenvalues and zero-order approximations for eigenvectors of $\boldsymbol{M}$. The resulting eigenvalues, to first order, are:

* By inversion of the matrix relationship (11), it is possible to express the initial coherences $\rho_k(0)$ as the sum over evolving components $\rho_j(t)$. The results of ref. 7 are presented in this form. However, the representation given by equation (12) is more logical and convenient for the analysis of experimental data.

$$\begin{aligned}
\lambda_1^{(1)} &= (\sqrt{2})\omega_1 \\
\lambda_2^{(1)} &= -(\sqrt{2})\omega_1 \\
\lambda_3^{(1)} &= \lambda_4^{(1)} = \lambda_5^{(1)} = 0 \\
\lambda_6^{(1)} &= -2\omega_Q + \omega_1/\sqrt{2} \\
\lambda_7^{(1)} &= -2\omega_Q - \omega_1/\sqrt{2} \\
\lambda_8^{(1)} &= 2\omega_Q - \omega_1/\sqrt{2} \\
\lambda_9^{(1)} &= 2\omega_Q + \omega_1/\sqrt{2}
\end{aligned} \tag{14}$$

Thus, in the first approximation we expect that the irradiated line of the **I** = 1 doublet would split into three components (0, ±(√2) ω_1). The other line of the **I** = 1 doublet would split into two components ($-2\omega_Q \pm \omega_1/\sqrt{2}$), and the 'mirror image' of this pair, in principle, would exist at ($2\omega_Q \pm \omega_1/\sqrt{2}$). This result is equivalent to that of Bowden *et al.*[7] It corresponds also to the Taylor expansion to order (ω_1/ω_Q) of the exact eigenvalues of Appendix A.

Eigenvectors, to zero order, are in columns:

$\eta^{1(0)}$	$\eta^{2(0)}$	$\eta^{3(0)}$	$\eta^{4(0)}$	$\eta^{5(0)}$	$\eta^{6(0)}$	$\eta^{7(0)}$	$\eta^{8(0)}$	$\eta^{9(0)}$
½	½	½	½	0	0	0	0	0
-½	½	½	-½	0	0	0	0	0
½	-½	½	-½	0	0	0	0	0
-½	-½	½	½	0	0	0	0	0
0	0	0	0	1	0	0	0	0
0	0	0	0	0	√½	√½	0	0
0	0	0	0	0	√½	-√½	0	0
0	0	0	0	0	0	0	√½	√½
0	0	0	0	0	0	0	√½	-√½

(15)

In order to calculate the line intensities we refer to equation (12). By recalling that the detectable signal is given by $\langle \mathbf{I}_- \rangle \propto (\hat{\rho}_{-10} + \hat{\rho}_{01})$ and assuming general initial conditions, the first-order perturbation results for line intensities are found:

$$\begin{aligned}
I^{(0)}[(\sqrt{2})\,\omega_1] &= \tfrac{1}{2}\,\{\rho_{-1-1}(0) - \rho_{00}(0) + \rho_{-10}(0) - \rho_{0-1}(0)\} \\
I^{(0)}[-(\sqrt{2})\,\omega_1] &= \tfrac{1}{2}\,\{-\rho_{-1-1}(0) + \rho_{00}(0) + \rho_{-10}(0) - \rho_{0-1}(0)\} \\
I^{(0)}[0] &= \{\rho_{0-1}(0) + \rho_{-10}(0)\} \\
I^{(0)}[-2\omega_Q + \omega_1/\sqrt{2}] &= \{\rho_{01}(0) + \rho_{-11}(0)\} \\
I^{(0)}[-2\omega_Q - \omega_1/\sqrt{2}] &= \{\rho_{01}(0) - \rho_{-11}(0)\} \\
I^{(0)}[2\omega_Q - \omega_1/\sqrt{2}] &= 0 \\
I^{(0)}[2\omega_Q + \omega_1/\sqrt{2}] &= 0
\end{aligned} \tag{16}$$

Since the degeneracies are removed by the first-order perturbation treatment, the second-order corrections arising from interactions between the $\boldsymbol{M}_{\mathrm{BD}}$ blocks may be handled within the framework of ordinary perturbation theory:

$$\lambda_n^{(\mathrm{cor})} = \Sigma_{k \neq n} \{N'_{nk} N'_{kn} / (\lambda_n^{(1)} - \lambda_k^{(1)})\} \tag{17}$$

where $\boldsymbol{N'}$ represents the $\boldsymbol{M'}$ perturbation after being transformed to the basis of zero-order eigenvectors $\boldsymbol{\eta}^{(0)}$:

$$\boldsymbol{N'} = \boldsymbol{U}^{(0)-1} \boldsymbol{M'} \boldsymbol{U}^{(0)} \tag{18}$$

This gives the following results for the eigenvalues (or frequencies) to second order from perturbation theory:

$$\begin{aligned}
\lambda_1^{(2)} &= (\sqrt{2})\,\omega_1 - (\sqrt{2})\,\omega_1 \epsilon \\
\lambda_2^{(2)} &= -(\sqrt{2})\,\omega_1 + (\sqrt{2})\,\omega_1 \epsilon \\
\lambda_3^{(2)} &= \lambda_4^{(2)} = \lambda_5^{(2)} = 0 \\
\lambda_6^{(2)} &= -2\omega_Q + \omega_1/\sqrt{2} - (6\omega_Q + \omega_1/\sqrt{2})\epsilon \\
\lambda_7^{(2)} &= -2\omega_Q - \omega_1/\sqrt{2} - (6\omega_Q - \omega_1/\sqrt{2})\epsilon \\
\lambda_8^{(2)} &= 2\omega_Q - \omega_1/\sqrt{2} + (6\omega_Q + \omega_1/\sqrt{2})\epsilon \\
\lambda_9^{(2)} &= 2\omega_Q + \omega_1/\sqrt{2} + (6\omega_Q - \omega_1/\sqrt{2})\epsilon
\end{aligned} \tag{19}$$

where $\epsilon = \omega_1^2/2(8\omega_Q^2 - \omega_1^2)$.

Table 1 illustrates the agreement between the theoretical estimations and experimentally observed frequencies obtained from an on-resonance Raman n.m.r. experiment with all pulses at ω_Q (Fig. 1). For ω_1 actually used in experiments, ϵ is a small quantity and second-order corrections are small even for $\omega_1 = \omega_Q/2$, being less than 6%. However, this order of perturbation treatment is important for the calculation of the eigenvectors (or intensities), since, at the preceding stage, the eigenvectors are calculated to zeroth order in ω_1. The calculation is standard:

$$\boldsymbol{\eta}^{n\,(\mathrm{cor})} = \Sigma_{k \neq n} \boldsymbol{\eta}^{k\,(0)} N'_{kn} / (\lambda_n^{(1)} - \lambda_k^{(1)}) \tag{20}$$

The first-order eigenvectors obtained in this way, but not reported here, can be used to derive the expressions for line intensities on the basis of equation (12):

$$\begin{aligned}
I^{(1)}[-(\sqrt{2})\omega_1] = {} & \tfrac{1}{4}(1+\beta)\{-\rho_{00}(0) - \rho_{0-1}(0) + \rho_{-10}(0) + \rho_{-1-1}(0) \\
& + \beta\rho_{01}(0) - \beta\rho_{-11}(0) + \alpha\rho_{10}(0) + \alpha\rho_{1-1}(0)\}
\end{aligned}$$

$$\begin{aligned}
I^{(1)}[(\sqrt{2})\omega_1] = {} & \tfrac{1}{4}(1-\alpha)\{\rho_{00}(0) - \rho_{0-1}(0) + \rho_{-10}(0) + \rho_{-1-1}(0) \\
& - \alpha\rho_{01}(0) - \alpha\rho_{-11}(0) - \beta\rho_{10}(0) + \beta\rho_{1-1}(0)\}
\end{aligned}$$

$$\begin{aligned}
I^{(1)}[0] = {} & \tfrac{1}{4}\{(1-\beta)(\rho_{00}(0) + \rho_{0-1}(0) + \rho_{-10}(0) + \rho_{-1-1}(0) \\
& - \beta\rho_{01}(0) - \beta\rho_{-11}(0) - \beta\rho_{10}(0) - \beta\rho_{1-1}(0)) \\
& + (1+\alpha)(-\rho_{00}(0) + \rho_{0-1}(0) + \rho_{-10}(0) - \rho_{-1-1}(0) \\
& + \alpha\rho_{01}(0) - \alpha\rho_{-11}(0) + \rho_{10}(0) - \alpha\rho_{1-1}(0)) \\
& + (\alpha+\beta)(2\rho_{11}(0) + (\alpha+\beta)\rho_{01}(0) + (\beta-\alpha)\rho_{-11}(0) \\
& + (\alpha+\beta)\rho_{10}(0) + (\beta-\alpha)\rho_{1-1}(0))\}
\end{aligned}$$

$$\begin{aligned}
I^{(1)}[-2\omega_Q + (\sqrt{\tfrac{1}{2}})\omega_1] = {} & \tfrac{1}{4}(1 + \tfrac{1}{2}(\alpha+\beta))\{(\alpha+\beta)\rho_{00}(0) \\
& + (\beta-\alpha)\rho_{0-1}(0) + (\alpha+\beta)\rho_{-10}(0) \\
& + (\beta-\alpha)\rho_{-1-1}(0) \\
& - 2\beta\,\rho_{11}(0) + 2\,\rho_{01}(0) + 2\rho_{-11}(0)\}
\end{aligned}$$

$$I^{(1)}[-2\omega_Q-(\sqrt{1/2})\omega_1] = \tfrac{1}{4}(1-\tfrac{1}{4}(\alpha+\beta))\{(\alpha+\beta)\rho_{00}(0) + (\beta-\alpha)\rho_{0-1}(0)-(\alpha+\beta)\rho_{-10}(0) -(\beta-\alpha)\rho_{-1-1}(0)-2\alpha\rho_{11}(0) +2\rho_{01}(0)-2\rho_{-11}(0)\}$$

$$I^{(1)}[2\omega_Q-(\sqrt{1/2})\omega_1] = -\tfrac{1}{4}(\tfrac{1}{2}(\alpha-\beta))\{(\alpha+\beta)\rho_{00}(0) +(\alpha+\beta)\rho_{0-1}(0)+(\beta-\alpha)\rho_{-10}(0) +(\beta-\alpha)\rho_{-1-1}(0)-2\beta\rho_{11}(0) +2\rho_{10}(0)+2\rho_{1-1}(0)\}$$

$$I^{(1)}[2\omega_Q+(\sqrt{1/2})\omega_1] = -\tfrac{1}{4}(\tfrac{1}{2}(\alpha-\beta))\{(\alpha+\beta)\rho_{00}(0) -(\alpha+\beta)\rho_{0-1}(0)+(\beta-\alpha)\rho_{-10}(0) -(\beta-\alpha)\rho_{-1-1}(0)-2\alpha\rho_{11}(0) +2\rho_{10}(0)-2\rho_{1-1}(0)\} \quad (21)$$

where $\alpha = \omega_1/(2(\sqrt{2})\omega_Q+\omega_1)$ and $\beta = \omega_1/(2(\sqrt{2})\omega_Q-\omega_1)$. Notice, that first-order eigenvectors along with the second-order eigenvalues of equations (19) can be substituted into equation (12) in accordance with our previous discussion.

In order to analyse the line intensities for our particular experiment we have to specify the initial conditions (i.e., density matrix elements $\rho_{MM'}(0)$). For a 2Q experiment, a sequence of non-selective pulses with $\Delta\omega \neq \pm\omega_Q$ has values:

$$\rho_{-1-1}(0) = \rho_{00}(0) = \rho_{11}(0) \neq 0$$
$$\rho_{1-1}(0) = -\rho_{-11}(0) \neq 0$$
$$\rho_{0-1}(0) = \rho_{-10}(0) = \rho_{01}(0) = \rho_{10}(0) = 0 \quad (22)$$

Inserting the results (22) in the general expressions (21) for line intensities we find immediately that for the case of a pure 2Q initial state the spectrum consists of two strong lines of slightly different height centred at $-2\omega_Q$, and two weak satellites of equal height centred at zero. Similar results are also obtained for CW irradiation without the preparation period,[20] i.e., with zero-quantum polarization as the starting condition.

$$\phi^1_0(0) = -i\sqrt{(3/2)}\,(\hat{\rho}_{-1-1}(0)-\hat{\rho}_{11}(0)) \neq 0 \quad (23)$$

where ϕ^1_0 is a component of the first-rank tensor ϕ^1.

In general, it may be desirable to express the initial and final states of the system $\boldsymbol{\rho}(0)$ and $\boldsymbol{\rho}(t)$ in terms of spherical tensors ϕ and then convert these into the $|M\rangle\langle M'|$ basis in order to apply equations (21) or to transform equations (21) to a spherical basis. The relationship between spherical tensors and $|M\rangle\langle M'|$ operators is given in Appendix B.

Results and Discussion

An on-resonance Raman n.m.r. experiment was performed using a system of two dipolar coupled spin ½ nuclei, i.e.,^{19}F of difluorotetrachloroethane aligned in a liquid crystal. The effective splitting was equivalent to ω_Q = 505 Hz. The results obtained for three ω_1 intensities, 97, 188 and 381 Hz, are shown in Fig. 1. Observed frequencies agreed well with the predictions of analytic treatment, equations (A4) and (A5), as well as perturbation approximations, equations (14) and (19) (see Table 1).

A consistent interpretation for observed line intensities is achieved only if some zero-quantum polarization is produced during the preparation period and r.f. leakage from the ^{19}F transmitter into the receiver coil contributes to the signal at zero frequency.

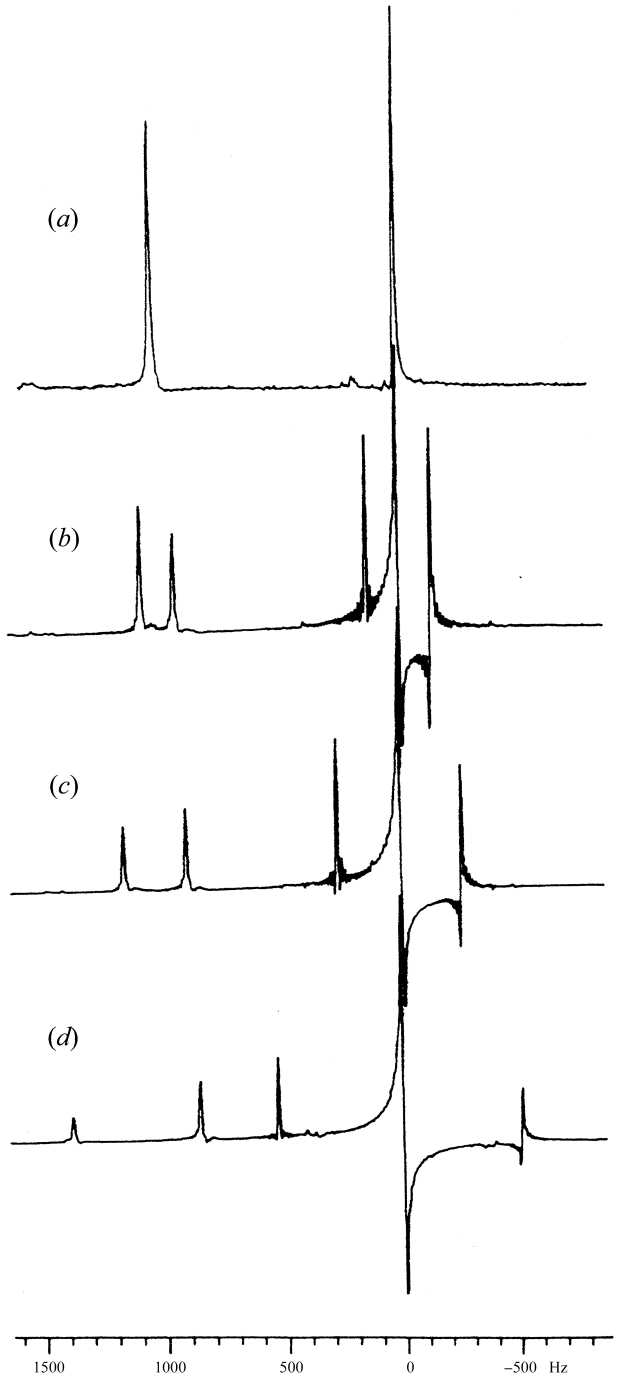

Fig. 1. (*a*) The steady-state spectrum of two coupled spins ½; (*b*)–(*d*) the spectra obtained following on-resonance Raman experiments for ω_1 97, 188 and 381 Hz respectively. The CW excitation is applied to the higher-field line of the dipolar doublet. Dipolar splitting is $2\omega_Q$ = 1010 Hz, and the splitting due to probing field is given by $(\sqrt{2})\omega_1$ and $\omega_1/\sqrt{2}$.

We consider the case of selective irradiation of one 1Q transition as a special case of an on-resonance Raman experiment. If selective CW irradiation is applied to one peak of a dipolar pair, then, as we have shown in this work, a strong peak (split by ω_1) arises at $-2\omega_Q$, together with three other relatively weak lines, their intensity reduced by the factor (ω_1/ω_Q) and $(\omega_1/\omega_Q)^2$. From Table 1, it is seen that the splitting produced for each peak of the dipolar doublet by the CW r.f. field is $(\sqrt{2})\omega_1$ and $\omega_1/\sqrt{2}$, respectively. Hence, the on-resonance Raman technique provides an easy way of measuring the strength of weak r.f. fields used for selective n.m.r. excitation.

Table 1. Spectrum frequencies in Hz as obtained for the sample in Fig. 1 with ω_Q = 505 Hz for three different magnitudes of probing field ω_1

ω_1 (Hz)	First-order perturbation	Second-order perturbation	Exact calculation	Experimental result
97	–1079	–1085	–1085	–1087
	–941	–949	–949	–949
	–137	–137	–137	–141
	137	137	137	131
188	–1143	–1168	–1168	–1169
	–877	–905	–904	–904
	–266	–263	–264	–268
	266	263	264	268
381	–1279	–1385	–1380	–1375
	–741	–867	–855	–853
	–539	–518	–525	–530
	539	518	525	519

On-resonance Raman n.m.r. may be regarded as the selective irradiation of a 1Q transition, and provides the basis for an interesting parallel. One method of creating MQ coherence is to use a sequence of non-selective pulses as described above. Another method is selective excitation of a certain transition where initial zero-quantum polarization is converted into observable 1Q coherences and, then, to MQ coherences. This method is usually described in terms of a selective pulse sequence,[1,21] but CW irradiation is essentially the same. In the Raman on-resonance experiment, selective excitation is used in reverse, i.e., to convert initially unobservable coherences into observable 1Q coherence. Thus, the method originally used for excitation of MQ coherences can be used in Raman experiments for detection of MQ coherences.

The criterion for the application of the present theoretical approach is based on an estimation of the parameter

$$\gamma = \min\{\omega_1/(\omega_Q - \Delta\omega), \omega_1/(\omega_Q + \Delta\omega)\} \qquad (24)$$

If γ is small, $\gamma \ll 1$, then ordinary perturbation theory is applicable. This can be referred to as a 'true' off-resonance case. If the condition $\gamma \ll 1$ does not hold, i.e., near-resonance condition, then degenerate perturbation theory is required. Near-resonance or off-resonance Raman experiments allow the detection of MQ lines in a single-shot experiment without the need for 2D experiments, providing both efficient coherence transfer and separate detection of 2Q and 1Q signals. The method presented in this paper may be applied to the case of near-resonance excitation, where the states are close to degeneracy and the condition $\gamma \ll 1$ is violated.

Experimental

The 1Q transitions were first observed in a three-level n.m.r. system consisting of two identical ^{19}F spins and subsequently an on-resonance Raman experiment was carried out. 2,2-Difluoro-1,1,1,2-tetrachloroethane (96%) was purchased from Aldrich Chemical Company, Inc., Milwaukee, Wisconsin, U.S.A., and dissolved 3–5% (v/v) in a nematic liquid crystal solvent (Nematic Phase ZLI-1083 Licristal from E. Merck, Darmstadt, Germany). For higher concentrations of solute (5–7.5%), the temperature was lowered from 297 to 277 K, to ensure the sample was below the isotropic phase transition or clearing point of the liquid crystal. The liquid crystal aligns in the external magnetic field (1.4 T) used for the n.m.r. experiment. The dipolar interaction between the ^{19}F spins is not averaged to zero because the solute orients in the liquid crystal.[5]

The on-resonance experiment was performed by using a modified TT-14 pulse spectrometer, operating at 56.4 MHz for fluorine. The experiment was carried out in CW mode with a cross-coil probe. The inner solenoidal coil was used for the non-selective hard pulse pair and detection, and the outer saddle coil was used for the weak probe field. The intensity of the CW radiofrequency was measured by using the same power in a straightforward nutation experiment.[22] This involved applying a long CW pulse to the single line of the ^{19}F resonance in the C_6F_6 spectrum, and Fourier transforming to obtain the nutation frequency. This was done at r.f. field strengths reduced by 36, 30, 24 and 18 dB relative to an arbitrary transmitter setting. Fluorine $\pi/2$ pulses of 3 μs, and CW r.f. field strengths of 100–500 Hz were used. Typically, a 25–50 ms acquisition period and 2 s repetition delay were used, with a 2 Hz line broadening applied to the resultant data before Fourier transformation. An acquisition time of 72 ms was used to record the spectrum of Fig. 1.

The narrowest line width observed was 10 Hz, which indicated a spin–spin or transverse relaxation time of longer than 200 ms. Variations in the degree of solute orientation and field inhomogeneity led to broader lines of 25–30 Hz. The longitudinal relaxation time, T_1, was measured by using an inversion recovery pulse sequence, and was determined to be *c*. 800 ms. Therefore, the relaxation effects during the acquisition period can be disregarded.

For the preparation of 2Q coherence, the delays between the hard pulses were calculated by using the measured doublet splittings. For the two-spin system, the splitting was *c*. 1010 Hz, and a delay of 495 μs was used. The splittings (and line widths), however, varied depending on the alignment of the liquid crystal. Hence a certain amount of zero-quantum polarization could be preserved during the preparation period.

Acknowledgment

We are indebted to Dr C. S. Yannoni, IBM Almaden Research Centre (U.S.A.), for help with the n.m.r. spectra and useful discussions.

References

[1] Ernst, R. R., Bodenhausen, G., and Wokaun, A., 'Principles of Nuclear Magnetic Resonance in One and Two Dimensions' (Oxford University Press: Oxford 1987).
[2] Anderson, W. A., *Phys. Rev*., 1956, **104**, 850.
[3] Yatsiv, S., *Phys. Rev*., 1959, **113**, 1522.
[4] Bodenhausen, G., *Prog. NMR Spectrosc*., 1981, **14**, 137.
[5] Yannoni, C. S., Kendrick, R. D., and Wang, P. K., *Phys. Rev. Lett*., 1987, **58**, 345.
[6] Bowden, G. J., Hutchison, W. D., and Separovic, F., *J. Magn. Reson*., 1988, **79**, 413.
[7] Bowden, G. J., Khachan, J., and Martin, J. P. D., *J. Magn. Reson*., 1989, **83**, 79.
[8] Yang, D., and Ye, C., *Chem. Phys. Lett*., 1990, **173**, 216.
[9] Yang, D., and Ye, C., *J. Magn. Reson*., 1992, **97**, 271.

[10] Yang, D., and Ye, C., *Acta Phys. Sin.*, 1991, **40**, 1533.
[11] Sanctuary, B. C., *Mol. Phys.*, 1983 **49**, 785.
[12] Ottiger, M., and Bax, A., *J. Biomol. NMR*, 1998, **12,** 361.
[13] Keller, A., *Adv. Magn. Reson.*, 1988, **12**, 183.
[14] Vega, S., and Pines, A., *J. Chem. Phys.*, 1977, **66**, 5624.
[15] Wokaun, A., and Ernst, R. R., *J. Chem. Phys.*, 1977, **67**, 1752.
[16] Fano, U., *Rev. Mod. Phys.*, 1957, **29**, 74.
[17] Vega, S., *J. Chem. Phys.*, 1978, **68**, 5518.
[18] Messiah, A., 'Quantum Mechanics' Ch. 26 (North Holland: Amsterdam 1969).
[19] Landau, L. D., and Lifshitz, E. M., 'Quantum Mechanics, Non-Relativistic Theory' Ch. 6 (Pergamon: Oxford 1977).
[20] Yannoni, C. S., personal communication.
[21] Hatanaka, H., Terao, T., and Hashi, T., *J. Phys. Soc. Jpn*, 1975, **39**, 835.
[22] Horne, D., Kendrick, R. D., and Yannoni, C. S., *J. Magn. Reson.*, 1983, **52**, 299.
[23] Sanctuary, B. C., *Mol. Phys.*, 1983, **49**, 1155.

Appendix A: Eigenvalues of $\boldsymbol{M}$

To find the eigenvalues of $\boldsymbol{M}$, it is necessary to solve the polynomial:

$$\lambda^3 [\lambda^6 - 2(4\omega_Q^2 + 3\omega_1^2)\lambda^4 + (4\omega_Q^2+3\omega_1^2)^2 \lambda^2 - \omega_1^2 (32\omega_Q^4+13\omega_Q^2\omega_1^2+4\omega_1^4)] = 0 \quad \text{(A1)}$$

Obviously, this has three eigenvalues of 0, and we must determine the other six. If we let $\Lambda = \lambda^2$, then it remains to solve the following cubic:

$$\Lambda^3 - 2(4\omega_Q^2+3\omega_1^2)\Lambda^2 + (4\omega_Q^2+3\omega_1^2)^2\Lambda - \omega_1^2(32\omega_Q^4+13\omega_Q^2\omega_1^2+4\omega_1^4) = 0 \quad \text{(A2)}$$

Thus, providing $0 < \omega_1 < 0.853\omega_Q$ and in practice $(\sqrt{2})\omega_1 < \omega_Q$, the solution can be written in the form:

$$\Lambda_1 = {}^2/_3 (4\omega_Q^2 + 3\omega_1^2) [1+\cos(\phi/3)]$$
$$\Lambda_2 = {}^2/_3 (4\omega_Q^2 + 3\omega_1^2) [1-\cos((\phi+\pi)/3)]$$
$$\Lambda_3 = {}^2/_3 (4\omega_Q^2 + 3\omega_1^2) [1-\cos((\phi-\pi)/3)] \quad \text{(A3)}$$

where

$$\phi = \cos^{-1}\{(-128\omega_Q^6+576\omega_Q^4\omega_1^2+135\omega_Q^2\omega_1^4+54\omega_1^6)/2(4\omega_Q^2+3\omega_1^2)^3\}$$
$$= \cos^{-1}\{(-128+576(\omega_1/\omega_Q)^2+135(\omega_1/\omega_Q)^4+54(\omega_1/\omega_Q)^6)/(128+288(\omega_1/\omega_Q)^2+218(\omega_1/\omega_Q)^4+54(\omega_1/\omega_Q)^6)\} \quad \text{(A4)}$$

Thus, the nine eigenvalues of $\boldsymbol{M}$ are:

$$\lambda_0 = 0,0,0$$
$$\lambda_{1,2} = \pm\sqrt{\{{}^2/_3 (4\omega_Q^2+3\omega_1^2) [1+\cos(\phi/3)]\}}$$
$$\lambda_{3,4} = \pm\sqrt{\{{}^2/_3 (4\omega_Q^2+3\omega_1^2) [1-\cos((\phi+\pi)/3)]\}}$$
$$\lambda_{5,6} = \pm\sqrt{\{{}^2/_3 (4\omega_Q^2+3\omega_1^2) [1-\cos((\phi-\pi)/3)]\}} \quad \text{(A5)}$$

Appendix B: $|M\rangle\langle M'|$ Operator Basis and Multipole Representation

The multipole representation $Y_q^k(\mathbf{I})$ is:[23]

$$Y_q^k(\mathbf{I}) = (\mathrm{i})^k [(2\mathbf{I}+1)(2k+1)]^{1/2} \times \Sigma_{MM'} (-1)^{\mathbf{I}-M} \begin{vmatrix} I & k & I \\ -M & q & M' \end{vmatrix} |IM\rangle\langle IM'| \quad \text{(B1)}$$

For $\mathbf{I} = 1$, the Y_q^k in the $|M\rangle\langle M'|$ representation are:

$$Y_0^0 = |-1\rangle\langle -1| + |0\rangle\langle 0| + |1\rangle\langle 1|$$
$$= \hat{\rho}_{-1-1}+\hat{\rho}_{00}+\hat{\rho}_{11}$$
$$Y_0^1 = -\mathrm{i}(\sqrt{(3/2)})\{|-1\rangle\langle -1| - |1\rangle\langle 1|\}$$
$$= -\mathrm{i}(\sqrt{(3/2)})\{\hat{\rho}_{-1-1}-\hat{\rho}_{11}\}$$
$$Y_{-1}^1 = \mathrm{i}(\sqrt{(3/2)})\{-|1\rangle\langle 0| + |0\rangle\langle 1|\}$$
$$= \mathrm{i}(\sqrt{(3/2)})\{\hat{\rho}_{-10}+\hat{\rho}_{01}\}$$
$$Y_1^1 = -\mathrm{i}(\sqrt{(3/2)})\{|0\rangle\langle -1| + |1\rangle\langle 0|\}$$
$$= \mathrm{i}(\sqrt{(3/2)})\{\hat{\rho}_{0-1}+\hat{\rho}_{10}\}$$
$$Y_0^2 = -(\sqrt{½})\{|-1\rangle\langle -1| - |0\rangle\langle 0| + |1\rangle\langle 1|\}$$
$$= -(\sqrt{(1/2)})\{\hat{\rho}_{-1-1}-2\hat{\rho}_{00}+\hat{\rho}_{11}\}$$
$$Y_{-1}^2 = (\sqrt{(3/2)})\{|-1\rangle\langle 0| - |0\rangle\langle 1|\}$$
$$= (\sqrt{(3/2)})\{\hat{\rho}_{-10}-\hat{\rho}_{01}\}$$
$$Y_1^2 = -(\sqrt{(3/2)})\{|0\rangle\langle -1| - |1\rangle\langle 0|\}$$
$$= -(\sqrt{(3/2)})\{\hat{\rho}_{0-1}-\hat{\rho}_{10}\}$$
$$Y_{-2}^2 = -(\sqrt{3})\{|-1\rangle\langle 1|\}$$
$$= -(\sqrt{3})\,\hat{\rho}_{-11}$$
$$Y_2^2 = -(\sqrt{3})\{|1\rangle\langle -1|\}$$
$$= -(\sqrt{3})\,\hat{\rho}_{1-1} \quad \text{(B2)}$$

The average multipoles $\phi_q^k = \langle Y_q^{k\,\dagger}\rangle$ are referred to as the polarizations.[23]

Donald W. Cameron to whom this issue has been dedicated.